PHYSICAL REVIEW A VOLUME 12, NUMBER 1

Energy and angular distribution of electrons ejected from helium by fast protons and electrons: Theory and experiment*

Steven T. Manson
Department of Physics, Georgia State University, Atlanta, Georgia 30303

L. H. Toburen
Battelle Pacific Northwest Laboratories, Richland, Washington 99352

D. H. Madison
Department of Physics and Physical Science, Drake University, Des Moines, Iowa 50311

N. Stolterfoht
Hahn-Meitner-Institut für Kernforschung Berlin Gmbh, Abteiling Strahlenphysik, West Berlin, Germany

(Received 27 February 1975)

A comprehensive study of the angular and energy distributions of electrons ejected in collisions of fast electrons and protons with He is presented. New experimental results for 300-keV, 1-MeV, and 5-MeV proton impact are reported along with theoretical results for 2-keV electron impact and 100-keV, 300-keV, 1-MeV, and 5-MeV proton impact. The theoretical results, based upon Born approximation with Hartree-Slater initial discrete and final continuum wave functions, show excellent agreement with experimental electron-impact results. Serious discrepancies are found between theory and experiment in the angular distribution of ejected electrons for forward angles for 100- and 300-keV proton impact; the discrepancies decrease markedly for 1-MeV proton impact and are absent for 5-MeV protons. The agreement between theory and experiment for intermediate and backward angles of electron ejection, on the other hand, is uniformly good for all proton impact energies. The reasons for this behavior in terms of a charge-exchange process to a continuum state contributing to electron ejection at forward angles is discussed, and the energy dependence of the data is shown to be consistent with this explanation.

I. INTRODUCTION

The ionization of atoms and molecules by fast charged particles is of importance in a number of areas including plasma physics, radiation physics, atmospheric physics and astrophysics, and in the study of penetration of charged particles through matter.[1-4] For the majority of applications the total ionization cross section is all that is required, but for a number of uses the energy and angular distributions of the ionized electrons are also necessary. In addition, from a theoretical point of view the basic quantity which is calculated is a triple differential cross section (TDCS), differential in the solid angle of the scattered particle, the solid angle of the ionized electron, and the energy lost by the scattered particle. Integration over the solid-angle distribution of the *scattered particle* yields the double differential cross section (DDCS), i.e., the energy and angular distribution of ionized electrons. Further, integration over the solid-angle distribution of the ionized electron gives the single differential cross section (SDCS), the energy distribution of ionized electrons. Finally, integration over ionized-electron energy yields the total ionization cross section. Each integration obliterates a great deal of detail so that ideally one would like to compare experiment and theory for the TDCS. This, however, is a difficult measurement and has only been carried out in a few cases.[5-12] These measurements are limited to incident electrons of fairly low energy and it is, at present, technologically unfeasible to perform these measurements with heavy incident particles such as protons owing to the smallness of the scattering angle. We have, therefore, chosen to study the DDCS, which is only a single integral over the most fundamental theoretical quantity.

Over the past decade, a number of measurements of the DDCS or energy and angular distributions of ejected electrons have appeared for proton[13-25] and electron[26-35] impact. These studies have been made for a number of target gases, but helium has been studied most owing to its simplicity. On the theoretical side, several Born approximation[35-38] and semiclassical[39] calculations have been carried out, all for protons on helium.

In this work, experimental and theoretical results from different laboratories are combined for

a comprehensive study of electron ejection in proton-helium collisions. In particular, measurements of H^+-He DDCS were extended to incident energies of 1 and 5 MeV at Battelle-Northwest (BNW) and the Hahn-Meitner Institute (HMI), respectively. In addition, results of Born-approximation calculations are presented for electron and proton impact on helium over a wide range of energies from 0.1 to 5 MeV using realistic discrete *and* continuum wave functions.

These studies have been carried out for a number of purposes. The first is to test the range of validity of the Born approximation through a systematic study over a wide range of incident-projectile energies and ionized-electron energies and angles. In particular, we wish to look at the large angles where previous calculations (with the exception of Ref. 38) have been inadequate and at the very small angles where a large maximum appears for the lower-energy incident protons.[13-17,40] Second, we wish to ascertain the accuracy of the calculation with a specific type of wave function so as to provide useful theoretical data for helium in ranges where experiment is difficult or unfeasible, and to build from these results a systematic theoretical approach for the other noble gases where experimental data is sparse. Finally, it is hoped that this study will focus attention on the remaining problems and stimulate further attempts at their solution.

In a sense, the theoretical part of this paper represents continuation of the work of Madison (Ref. 38). The differences include the facts that the scope of this paper is broader and the wave functions used are *slightly* different.

In Sec. II of the paper the theory and method of calculation are discussed. Section III contains some information on the experimental arrangement and an assessment of the accuracy of the results. In Sec. IV the experimental and theoretical data are presented, compared, and discussed. Section V presents our conclusions and final remarks along with some prospectus for further work.

II. THEORY AND METHOD OF CALCULATION

We consider a fast particle of charge ze, mass M, and initial momentum $\hbar\vec{k}_0$ (initial nonrelativistic kinetic energy $T=\hbar^2k_0^2/2M$) ionizing a stationary atom of atomic number Z. Let the energy of the ionized electron in rydbergs be ϵ/R and its momentum be $\hbar\vec{k}$ [$\epsilon/R=(ka_0)^2$, where a_0 is the Bohr radius]. Further, let the momentum of the scattered fast particle be $\hbar\vec{k}_f$ so that the momentum transfer $\hbar\vec{K}=\hbar\vec{k}_0-\hbar\vec{k}_f$. The triple differential cross section (TDCS) for this process, differential in the energy of the ionized electron ϵ (or, equivalently, the energy lost by the impinging fast particle $\epsilon+I$, where I is the ionization energy of the electron), differential in the direction of the ionized electron, and differential in the direction of the scattered particle, is given in Born approximation by[41,42]

$$\frac{\partial^3\sigma_{if}}{\partial(\epsilon/R)\partial\Omega_e\partial\Omega}=\frac{4\pi^2M^2z^2e}{h^4}\frac{k_f}{k_0}\left|\frac{4\pi}{K^2}\int\psi_f^*\sum_j e^{i\vec{K}\cdot\vec{r}_j}\psi_i\,d\tau\right|^2, \tag{1}$$

where ψ_i is the initial antisymmetric atomic wave function and ψ_f the final antisymmetric wave function with the continuum part normalized per unit energy in rydbergs, and $\partial\Omega_e$ and $\partial\Omega$ are the differential solid angles in the direction of the ionized electron and scattered particle, respectively; M and z are the mass and atomic number of the incident particle. If we express ψ_i and ψ_f as antisymmetric products of single-particle functions and assume no core relaxation, Eq. (1) reduces to

$$\frac{\partial^3\sigma_{nl_0m_0\epsilon\hat{k}}}{\partial(\epsilon/R)\partial\Omega_e\partial\Omega}=\frac{4M^2z^2e^2}{\hbar^4K^4}\frac{k_f}{k_0}\left|\int\psi_{\epsilon,\hat{k}}^*e^{i\vec{K}\cdot\vec{r}}\psi_{nl_0m_0}\,d\tau\right|^2, \tag{2}$$

where an electron with quantum numbers nl_0m_0 has been ionized.

The continuum wave, which asymptotically represents a Coulomb wave in the $\hat{k}$ direction, is given by[43]

$$\psi_{\epsilon,\hat{k}}=\sum_{l,m}i^le^{-i\xi_l}\frac{u_{\epsilon l}(r)}{r}Y_l^m(\hat{r})Y_l^m(\hat{K})^*, \tag{3}$$

with ξ_l the phase shift relative to plane waves and $u_{\epsilon l}(r)$ normalized per unit energy in rydbergs; the discrete function is of the form

$$\psi_{nl_0m_0}=\frac{u_{nl_0}(r)}{r}Y_{l_0}^{m_0}(\hat{r}). \tag{4}$$

Then, using the expansion

$$e^{i\vec{K}\cdot\vec{r}}=4\pi\sum_{\lambda,\mu}i^\lambda j_\lambda(Kr)Y_\lambda^\mu(\hat{r})Y_\lambda^\mu(\hat{K})^*, \tag{5}$$

with j_λ the spherical Bessel function of order λ, along with Eqs. (3) and (4), we find for the TDCS after suitable averaging over initial and summing over final degenerate magnetic substates (and after a liberal dose of angular momentum algebra)

$$\frac{\partial^3\sigma_{nl_0,\epsilon\hat{k}}}{\partial(\epsilon/R)\partial\Omega_e\partial\Omega}=\frac{z^2}{T/R}\frac{M}{m}\frac{N_{nl_0}}{\pi K^4}k_0k_f\sum_{l,l',\lambda,\lambda',L}i^{\lambda+\lambda'+l+l'}e^{i(\xi_l-\xi_{l'})}R^{\lambda}_{nl_0,\epsilon l}(K)R^{\lambda'}_{nl_0,\epsilon l'}(K)(2L+1)(2l+1)(2l'+1)$$
$$\times(2\lambda+1)(2\lambda'+1)\begin{pmatrix}l' & \lambda' & l_0\\ 0 & 0 & 0\end{pmatrix}\begin{pmatrix}l & \lambda & l_0\\ 0 & 0 & 0\end{pmatrix}\begin{pmatrix}l & l' & L\\ 0 & 0 & 0\end{pmatrix}\begin{pmatrix}\lambda & \lambda' & L\\ 0 & 0 & 0\end{pmatrix}$$
$$\times\begin{Bmatrix}\lambda & \lambda' & L\\ l' & l & l_0\end{Bmatrix}P_L(\cos\theta_{eK}), \tag{6}$$

where

$$R_{nl_0,\epsilon l}(K)=\int_0^\infty u_{\epsilon l}(r)^*j_\lambda(Kr)u_{nl_0}(r)\,dr, \tag{7}$$

m is the electron mass, N_{nl_0} is the number of electrons in the (nl_0) subshell initially, $\begin{pmatrix}a & b & c\\ d & e & f\end{pmatrix}$ is the Wigner 3-j symbol,[44] $\begin{Bmatrix}a & b & c\\ d & e & f\end{Bmatrix}$ is the Wigner 6-j symbol,[45] P_L is the Legendre polynomial of order L, and θ_{eK} is the angle between the ionized-electron direction $\hat{k}$, and the momentum-transfer vector $\vec{K}$.

Before proceeding, we make several observations concerning the structure of Eq. (6) for the TDCS. The momentum transfer $\vec{K}$ defines an axis of symmetry and the azimuthal angle about $\vec{K}$ does not enter into the TDCS expression. Thus, measurements out of the plane defined by the scattered particle can provide no new information, if the Born approximation applies. In particular, the TDCS remains the same for $\theta_{eK}\to-\theta_{eK}$ so that measurements on either side of the $\vec{K}$ direction should be the same and, in practice, provide a consistency check. Conversely, differing experimental results at different azimuthal angles (but constant θ_{eK}) imply a breakdown of the Born approximation. Another important feature of the TDCS is that it depends not only on the amplitudes of the various matrix elements, the R's, but also on the relative phases of the different continuum partial waves. Therefore, calculations which do a good job on the amplitudes but poorly on the phases are expected *a priori* to give poor results for the TDCS.

To obtain the DDCS, the energy and angular distribution of the ionized electrons, the TDCS must be integrated over the directions of the scattered particle, i.e.,

$$\frac{\partial^2\sigma_{nl_0,\epsilon\hat{k}}}{\partial(\epsilon/R)\partial\Omega_e}=\int\frac{\partial^3\sigma_{nl_0,\epsilon\hat{k}}}{\partial(\epsilon/R)\partial\Omega_e\partial\Omega}\,d\Omega. \tag{8}$$

This integration can be performed using the addition theorem for spherical harmonics,

$$P_L(\cos\theta_{eK})=\frac{4\pi}{2L+1}\sum_M Y_L^M(\hat{K})Y_L^M(\hat{k})^*, \tag{9}$$

where the z axis is now chosen to be parallel to the incident projectile direction k_0. Further, from the definition of momentum transfer,

$$K^2=k_0^2+k_f^2-2k_0k_f\cos\theta, \tag{10}$$

it follows that

$$K\,dK\,d\phi_K=k_0k_f\sin\theta\,d\theta\,d\phi=k_0k_f\,d\Omega. \tag{11}$$

Using Eqs. (6), (9), and (11) in Eq. (8) then, we obtain

$$\frac{\partial^2\sigma_{nl_0,\epsilon\hat{k}}}{\partial(\epsilon/R)\,d\Omega_e}=\frac{2z^2a_0^2}{T/R}\frac{M}{m}N_{nl_0}\sum_{l,l',\lambda,\lambda',L}i^{\lambda+\lambda'+l+l'}e^{i(\xi_l-\xi_{l'})}(2L+1)(2l+1)(2l'+1)(2\lambda+1)(2\lambda'+1)$$
$$\times\begin{pmatrix}l' & \lambda' & l_0\\ 0 & 0 & 0\end{pmatrix}\begin{pmatrix}l & \lambda & l_0\\ 0 & 0 & 0\end{pmatrix}\begin{pmatrix}l & l' & L\\ 0 & 0 & 0\end{pmatrix}\begin{pmatrix}\lambda & \lambda' & L\\ 0 & 0 & 0\end{pmatrix}$$
$$\times\begin{Bmatrix}\lambda & \lambda' & L\\ l' & l & l_0\end{Bmatrix}\left(\int_{K_{\min}}^{K_{\max}}P_L(\cos\theta_K)R^{\lambda}_{nl_0,\epsilon l}(K)R^{\lambda}_{nl_0,\epsilon l'}(K)\frac{d(Ka_0)}{(Ka_0)^3}\right)P_L(\cos\theta_e), \tag{12}$$

with

$$\cos\theta_K=\frac{K^2+k_0^2-k_f^2}{2k_0k_f}=\left((Ka_0)^2-\frac{M}{m}\frac{\Delta E}{R}\right)\left\{2\frac{M}{m}\left[\frac{T}{R}\left(\frac{T}{R}-\frac{\Delta E}{R}\right)\right]^{1/2}\right\}^{-1} \tag{13}$$

and $\Delta E=\epsilon+I$, the energy loss. The upper and lower limits of integration are obtained from Eq. (10) by setting $\theta=\pi$ and $\theta=0$, respectively. The dependence on relative phases of the various partial waves remains.

Since we are dealing with ionization from the ground state ($1s^2$) of He in this paper, it is instructive to point out the simplifications that occur for $l_0=0$, i.e., ionization of an s electron. In that case, all of the 3-j and 6-j symbols involving l_0 contract to a single number,[44,45] and angular momentum algebra shows that $\lambda=l$ and $\lambda'=l'$. The DDCS, Eq. (12), then becomes

$$\frac{\partial^2\sigma_{ns,\epsilon\hat{k}}}{\partial(\epsilon/R)\partial\Omega_e}=\frac{2z^2a_0^2}{T/R}\frac{M}{m}N_{nl_0}\sum_{l,l',L}\cos(\xi_l-\xi_{l'})(2L+1)(2l+1)(2l'+1)$$

$$\times\begin{pmatrix}l & l' & L\\ 0 & 0 & 0\end{pmatrix}^2\left(\int_{K_{\min}}^{K_{\max}}P_L(\cos\theta_K)R^l_{ns,\epsilon l}(K)R^{l'}_{ns,\epsilon l'}(K)\frac{d(Ka_0)}{(Ka_0)^3}\right)P_L(\cos\theta_e)\,, \qquad (14)$$

which is very much simpler to manage.

Integrating over the angular dependence of the ionized electrons yields the single differential cross section (SDCS), the energy spectrum of ionized electrons. The only term in the DDCS which depends on the electron ejection angle θ_e is $P_L(\cos\theta_e)$; integration over $d\Omega_e$ gives $4\pi\delta_{L,0}$, which obliterates all terms in Eq. (12) [or Eq. (14)] except $L=0$, giving

$$\frac{d\sigma_{nl_0,\epsilon\hat{k}}}{d(\epsilon/R)}=\frac{8\pi a_0^2z^2N_{nl_0}}{T/R}\frac{M}{m}$$

$$\times\sum_{l,\lambda}(2l+1)(2\lambda+1)\begin{pmatrix}l & \lambda & l_0\\ 0 & 0 & 0\end{pmatrix}^2$$

$$\times\int_{K_{\min}}^{K_{\max}}[R_{nl_0,\epsilon l}(K)]^2\frac{d(Ka_0)}{(Ka_0)^3}\,, \qquad (15)$$

which is a well-known result.[4,46,47] Note that the SDCS has no interference terms and thus, to get a reasonable result, one needs only to calculate the *magnitude* of the matrix elements well; their *phases* are irrelevant. We also note that one can arrive at Eq. (15) for the SDCS by alternate means via the inelastic cross section for the incident fast particle differential in scattering angle and energy loss, which is proportional to the generalized oscillator strength (GOS).[4,46,47]

In our calculations we have employed wave functions which are products of one-electron orbitals. The one-electron orbitals $u_{nl}(r)$ [Eq. (4)] for the initial discrete state of the electrons are of the Hartree-Slater [HS] form as tabulated by Herman and Skillman.[48] Each is a solution to the radial Schrödinger equation with the same central potential $V(r)$,

$$\left(\frac{d^2}{dr^2}+V(r)+\epsilon_{nl}-\frac{l(l+1)}{r^2}\right)u_{nl}(r)=0\,,$$

$$V(r)\to 2Z/r \quad \text{as } r\to 0, \qquad V(r)\to 2/r \quad \text{as } r\to\infty\,.$$

Here Z is the nuclear charge, ϵ_{nl} is the energy of an electron in the nlth subshell in rydbergs, and r is in units of a_0. The final continuum orbitals $u_{\epsilon l'}(r)$ [Eq. (3)] are taken to be solutions to the radial Schrödinger equation with the same central potential as the initial state,

$$\left(\frac{d^2}{dr^2}+V(r)+\epsilon-\frac{l'(l'+1)}{r^2}\right)u_{\epsilon l'}(r)=0\,, \qquad (17)$$

in which ϵ is the ionized-electron energy in rydbergs and $u_{\epsilon l'}$ is normalized such that

$$u_{\epsilon l'}(r)\underset{r\to\infty}{\sim}\pi^{-1/2}\epsilon^{-1/4}\sin[\epsilon^{1/2}r-\epsilon^{-1/2}\ln 2\epsilon^{1/2}r$$

$$-1/2\,l'\pi+\sigma_{l'}(\epsilon)+\delta_{l'}(\epsilon)]\,, \qquad (18)$$

where

$$\sigma_{l'}(\epsilon)=\arg\Gamma(l'+1-i\epsilon^{-1/2}) \qquad (19)$$

and $\delta_{l'}$ is the phase shift with respect to Coulomb waves.[49] The sum of $\sigma_{l'}$ and $\delta_{l'}$ is just the phase shift with respect to plane waves, ξ_l, defined in Eq. (3). This is the usual normalization of a continuum wave function per unit energy range. The orbitals of the initial-state atomic electrons not involved in the transition are assumed to be unchanged by the collision; i.e., we consider no core relaxation. The details of the numerical methods used to obtain and normalize the continuum wave functions are described in detail elsewhere.[46,50,51]

The summations over the continuum angular momentum channels (l and l') implied by the cross-section equations are, in principle, infinite. To perform the calculations, however, these sums must be truncated. This can be done with reasonable accuracy since the contributions to the cross sections eventually fall off with increasing continuum angular momentum. We have gone up to values of l and l' of 15 for a total of 16 continuum partial waves. This choice was dictated by the need for convergence to 5% at the highest ejected-electron energy reported of 48 Ry (652.8 eV).

III. EXPERIMENTAL TECHNIQUES AND COMPARATIVE RESULTS OF DIFFERENT LABORATORIES

Experimental results for 1- and 5-MeV proton impact on He were obtained at Battelle-Northwest

(BNW) and the Hahn-Meitner Institute (HMI), respectively. Further, at both laboratories, measurements using 300-keV protons were carried out to compare with experimental results obtained previously by Rudd *et al.*[14,15] A brief description and comparison of the various experimental techniques is given in the review article of Rudd and Macek.[52]

The high-energy measurements at HMI reported in this paper were made with the same apparatus used in previous work with low-energy protons and is described in detail elsewhere.[24] The apparatus was simply moved to a 7-MV Van de Graaff accelerator for the high-energy measurements. In brief, a magnetically analyzed and collimated beam of protons was crossed by an atomic beam *ejected* from a cylindrical tube connected with a gas reservoir. Electrons ejected from the scattering volume were detected by an electron multiplier after being analyzed by a parallel-plate electrostatic spectrometer.[53] The spectrometer had an angular acceptance of ±2.8°, an energy resolution of 2.6%, and could be positioned to detect electrons at angles from 22° to 152°. To place the results on an absolute scale, cross sections were also measured in auxiliary experiments with a well-known homogeneous pressure distribution in the scattering volume. Magnetic fields were reduced to a few milligauss by shielding with a Mu metal box the same size as the scattering chamber.

The measurements made at BNW were conducted using the apparatus described in detail in Ref. 18. A magnetically analyzed and collimated proton beam from a 2-MV Van de Graaff accelerator is passed through a differentially pumped target-gas cell and collected in a Faraday cup. Electrons ejected in ionizing collisions pass out of the gas cell through a slit, are electrostatically analyzed by a cylindrical mirror analyzer and are detected by a continuous channel electron multiplier. The electrostatic analyzer has an acceptance angle of approximately ±2°, an energy resolution of 3.5%, and can be remotely positioned to detect electrons at angles from 15° to 125°. Magnetic fields in the vicinity of the interaction region are reduced to a few milligauss by three mutually perpendicular sets of Helmholtz coils.

Since the experimental techniques used for the cross-section measurements at the different laboratories are quite different, a comparison of the cross sections measured at a common incident-particle energy was made to determine if there were systematic differences between the measurements. Figure 1 presents a comparison of the electron-energy spectra for electrons ejected at 50° by 0.3 MeV protons measured at HMI and BNW, as well as the previous data of Rudd *et al.*[15] A comparison of the angular distributions is shown for selected electron energies in Fig. 2.

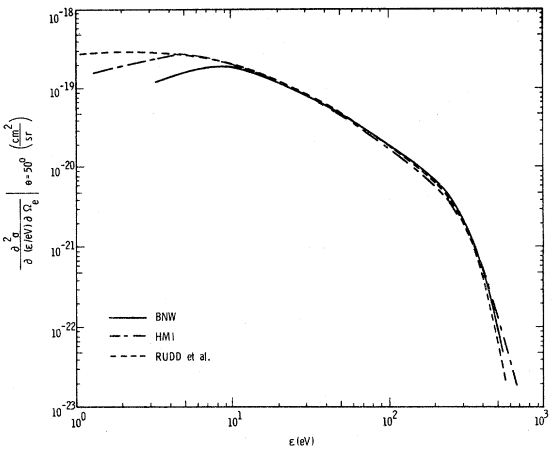

FIG. 1. Experimental double differential cross section (DDCS) for electrons ejected at 50° by 300-keV protons, on He, as a function of electron energy as measured at Battelle Northwest (BNW), Hahn-Meitner-Institut (HMI), and University of Nebraska (Ref. 15).

The agreement between the measurements of the different laboratories is quite good even though quite different techniques are employed. The largest discrepancies between the different measurements occur for low-energy electron emission where the experimental uncertainties are largest. A loss in transmission is normally expected for analysis of very-low-energy electrons by electrostatic energy analyzers due to fringing electrostatic fields and to the effects of residual magnetic fields. This is definitely noted for electron energies less than 20 eV in the Battelle-Northwest measurements and to some extent in the Hahn-Meitner work for electron energies below 3 eV. In the work of Rudd *et al.*, the low-energy electrons were accelerated before energy analysis to improve the electron transmission through the analyzer. The use of acceleration must be approached with care as this procedure may also introduce uncertainties in the measured cross sections due to the focusing properties of the accelerating fields. These focusing effects were particularly important in early results reported at HMI,[24,25] where preacceleration of low-energy electrons was used. The errors introduced in the first measurements of low-energy electron emission cross sections made at HMI have since been understood and attributed to focusing effects of the preacceleration voltages. By removing the preacceleration voltages the anomalously high cross sections for low-energy electron emission no longer occur and good agreement with other measurements is obtained, as is shown in Fig. 1.

The accuracy of our measured absolute cross

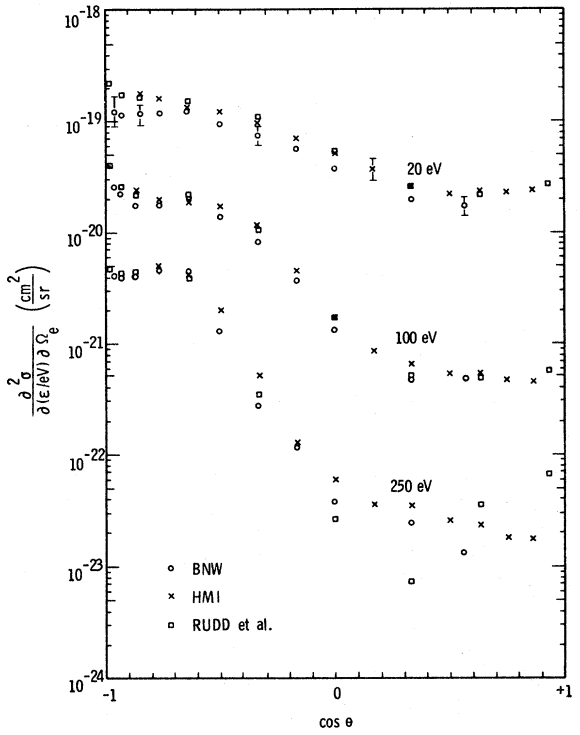

FIG. 2. Experimental double differential cross section (DDCS) for electrons ejected at 20, 100, and 250 eV by 300-keV protons on He as a function of angle as measured at Battelle Northwest (BNW), Hahn-Meitner-Institut (HMI), and University of Nebraska (Ref. 15).

sections is estimated as ±20% for electron energies above 20 eV. It should be noted that at the extreme high-energy end of each electron-energy spectrum the accuracy is somewhat poorer since the number of ejected electrons becomes small and ultimately cannot be separated from normal background count. This effect results in a statistical scatter in the cross sections at the extreme high-energy end of the spectrum greater than the ±20% uncertainty noted above. This is why one sees a large degree of scatter in the large-angle results plotted for 250-eV ejected electrons in Fig. 2. These electron energies occur at the upper end of the electron-energy spectra for electron ejection into large angles by 0.3-MeV protons. Below 20 eV the accuracy decreases due to the effects of stray magnetic and electric fields. Between 10 and 20 eV, error limits of 20 to 40% should be considered, and below 10 eV, cross sections are uncertain by as much as a factor of 2 or more. By observation of the close agreement illustrated in Fig. 1, for results of three quite different measurement techniques one may consider the 20% uncertainties as being overly cautious. However, for each technique there are uncertainties in detection efficiencies, target-pressure measurements, etc., which when honestly considered, result in the ±20% figure. It is hoped that the interlaboratory agreement is evidence that our quoted uncertainties are conservative and not purely coincidence.

IV. RESULTS AND DISCUSSION

We have measured the DDCS for 1- and 5-MeV proton impact on He and have performed calculations for 2-keV electron impact and 0.1-, 0.3-, 1-, and 5-MeV proton impact on He. The calculations were performed for ejected-electron energies from threshold to 652.8 eV ($\epsilon = 0$ to 48 Ry). We will discuss the electron-impact results first, since it is the simpler case. For incident electrons no charge-transfer channels exist as they do for proton impact and although we have neglected exchange this should be unimportant for ejection of low-energy electrons by 2-keV incident electrons.

A. 2-keV electron impact

The theoretical DDCS we have obtained are given in Fig. 3 for ejected electrons from threshold to 326.4 eV ($\epsilon = 0$ to 24 Ry). These angular distribu-

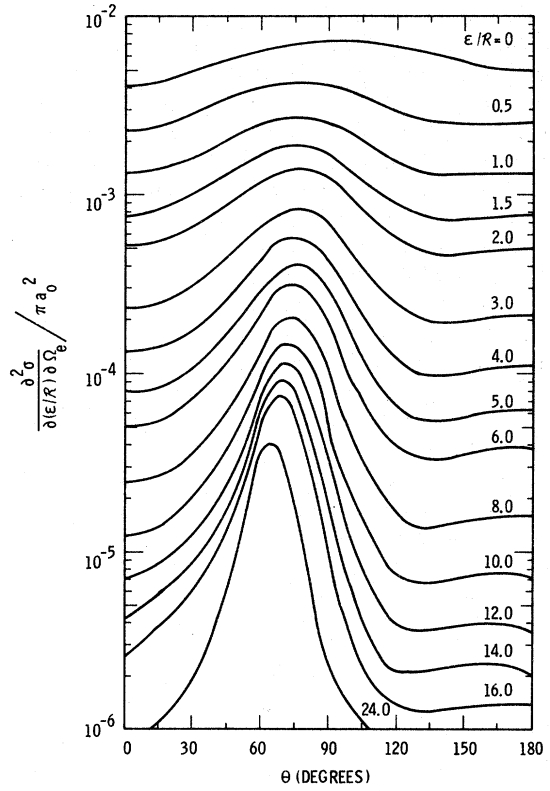

FIG. 3. Calculated angular distribution (DDCS) for electrons ejected at energies ϵ/R from 0 to 24 Ry by 2-keV electron-impact ionization of He.

tions change rather markedly with increasing ejected-electron energy: from a rather flat distribution at threshold, varying with angle by less than a factor of 2, to a very sharply peaked distribution at $\epsilon = 24$ Ry. The peaking at large ϵ can be explained by noting that classically, for collisions of a fast electron incident on a free electron initially at rest, the kinematics of the final state are completely determined. That is, for any given amount of energy transferred the target electron goes off in a well-defined direction giving a δ-function angular distribution. If, however, the target electron is bound, the binding gives it an initial momentum distribution (the absolute square of its wave function in momentum space) which changes the relative velocity of the incident and target electron. This "smears out" the δ-function distribution. For energy transfer large compared to the binding energy, the smearing out will be quite small and a sharply peaked angular distribution will occur. As can be seen in Fig. 3, the calculated quantum-mechanical angular distributions are becoming more classical (the peak is becoming sharper) with increasing ϵ. Conversely, for small energy transfer (and small ϵ) the smearing will flatten the angular distribution considerably. This, too, is borne out by the results in Fig. 3. This semiclassical picture of the collision forms the basis for the *binary-encounter approximation* (BEA)[39,54,55] and can be expected to be fairly reliable in the angular range about the peak in the DDCS.

From a quantum-mechanical viewpoint, the low-energy ejected electrons will have very little angular momentum. This means that for small ϵ the matrix element $R^{\lambda}_{nl_0,\epsilon l}(\epsilon)$ [Eq. (7)] is very small for all l's except for a few of the lowest values. Thus, from the expression for the DDCS, Eq. (14), the coefficient of $P_L(\cos\theta_e)$ is small unless L is small; i.e., only a few terms contribute to the summation. For the 1s of He, only $l = 0$, 1 contribute significantly at $\epsilon = 0$ ($l \geq 2$ continuum partial waves are kept out by the repulsive centrifugal barrier resulting in very little overlap with the discrete wave function). Thus, from Eq. (14), only P_0, P_1, and P_2 contribute significantly and the angular distribution is rather flat and characteristic of such contributions. For increasing ϵ, the higher-l continuum functions penetrate the atom and the matrix element at these l's becomes significant. In this case, quite a number of P_L's contribute to the sum and the angular distribution is sharply peaked.

From Eqs. (12) and (14) it is seen that theoretically the DDCS is expressed in terms of the Legendre polynomials, the P_L's. It would be very useful for experimentalists to characterize their data in this manner since comparison between individual partial waves could then be made. This, in turn, would enable one to isolate the continuum partial wave (or waves) that causes the discrepancy between theory and experiment. We intend to do this and the results will be presented in the future. From a theoretical standpoint, the coefficients of each $P_L(\cos\theta_e)$ term are first calculated, as prescribed in Eqs. (12) and (14) *and then* a summation is performed to obtain the DDCS. More information could be obtained if a comparison between the theoretical and experimental coefficients could be made and not just between the sums, i.e., the DDCS's.

The behavior of the DDCS for electron ejection at backward angles (Fig. 3) does not show a minimum at 180° (except just at threshold) as is characteristic of BEA results[39,54,55] and Born-approximation calculations which employ *hydrogenic* continuum functions.[36,37] In fact, our calculations give a large-angle DDCS which increases with angle and results in a local maximum either at 180° or just below 180°. The occurrence of this large-angle behavior in our results can be explained in the following way: In a charged-particle impact-ionization process, a bound nl electron undergoes a transition to a continuum $\epsilon l'$ state. This process, unlike photoionization, has no selection rules on the final angular momentum l'. Thus, the ejected electron can be in an ϵs, ϵp, ϵd, ϵf, ϵg, etc., final continuum state. These continuum waves interfere with each other so that the relative phases of each pair of continuum waves is important. This phase difference enters the DDCS expression [Eqs. (12) and (14)] as $\cos(\xi_l - \xi_{l'})$, where ξ_l and $\xi_{l'}$ are, respectively, the phase shifts of the ϵl and $\epsilon l'$ continuum wave functions with respect to plane waves. When all of the partial waves are in phase and interfere *con*structively, we get the "binary-encounter" peak discussed above. This is analogous to the central maximum in a diffraction pattern. At larger angles this interference is no longer totally constructive due to the variation of the P_L's with angle, and is getting less so rapidly. This leads to the rapid falloff of the DDCS with increasing angle above the peak. Eventually an angle is reached where the values of the P_L's are such that the various partial waves interfere destructively as much as they are going to, much like the first minimum in a diffraction pattern. At still larger angles, the DDCS *in*creases like the diffraction-pattern intensity going to the second maximum. It is clear that the details of the positions of the minima and backward-angle maxima depend very sensitively on the relative phases of the continuum partial waves. Thus, at $\epsilon = 0$, the DDCS shown in Fig. 3 simply flattens in the backward direction with the minimum at 180°; from

$\epsilon = 0.5$ to $\epsilon = 6$ a minimum appears and a secondary maximum occurs at 180°; for $\epsilon = 8$ to $\epsilon = 14$ the secondary maximum appears below 180°. All of this behavior is a consequence of the changing phase shifts of the continuum partial waves as a function of ejected-electron energy ϵ. BEA, being a semiclassical model, does not include these phase-shift effects and, thus, cannot be expected to represent the DDCS accurately at large angles where they become important.[39] Hydrogenic Born calculations include only the Coulomb phase shift [Eq. (19)]. Since this approximation neglects the non-Coulomb phase shift $\delta_l(\epsilon)$ [Eq. (18)], it too is rather poor at large angles.[36,37] It was shown, however, that such a calculation, employing a Hartree-Fock function for the continuum p wave only, did fairly well at the backward angles,[37] thus illustrating the importance of the non-Coulomb phase shifts.

To get a feeling for the accuracy of our results, we show the calculated DDCS's along with the experimental data of Opal, Beaty, and Peterson[28-31] in Fig. 4A–4D for ejected-electron energies of 13.6, 40.8, 81.6, and 163.2 eV. The striking feature of this comparison is the excellent agreement between theory and experiment over the entire range of ϵ considered. The only significant deviations occur at $\theta = 30°$ and 150°, the smallest and largest experimental angles.[28-31] It is possible that these discrepancies represent experimental rather than theoretical difficulties. In the experiment a simple $\sin\theta$ correction was used to account for the influence of angular changes in the effective length of the interaction region. In all likelihood, this first-order approximation becomes poorer as θ moves away from 90° and higher-order corrections become important. This correction term would result in the DDCS vanishing at $\theta = 0°$ and 180°, which is clearly incorrect. Thus, we feel it represents an over-correction and yields cross sections at 30° and 150° which are too small. This conclusion is further supported by a recent experiment of Crooks and Rudd,[35] who measured the DDCS for electron impact on He at incident energies of 50–400 eV and found that their results were uniformly higher at 30° and 150° when compared with the results of Refs. 28–31.

Integrating over the angle, the energy distribution of ejected electrons, or SDCS, is obtained. Our result is shown in Fig. 5 along with the experimental results.[28-31] The agreement is seen to be excellent except for $\epsilon \leq 13$ eV, where the experimental results lie below the theoretical by as much as 20% (for the lowest-energy ejected electron measured). Further, this discrepancy appears to be increasing with decreasing ϵ to perhaps as much as 40% at $\epsilon = 0$. We can ascertain the correct value of the SDCS at $\epsilon = 0$ from Kim and Inokuti,[56] who extrapolated upward from very accurate re-

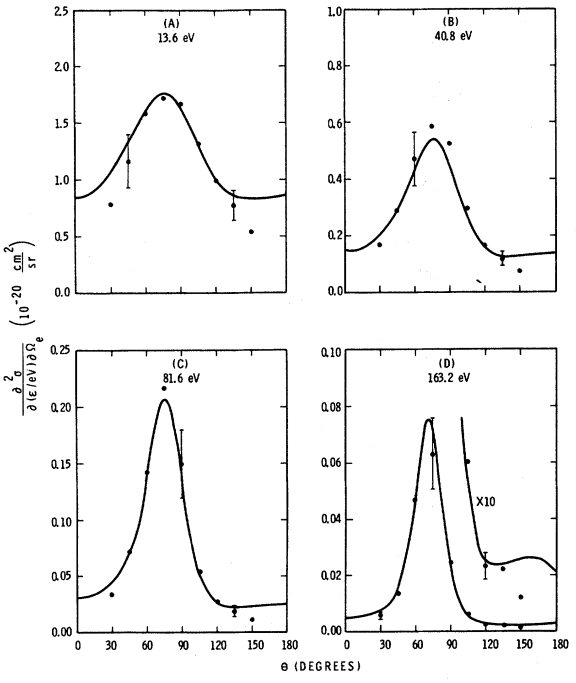

FIG. 4. Angular distribution (DDCS) for electrons ejected at 13.6, 40.8, 81.6, and 163.2 eV by 2-keV electron impact on He. Solid curves, calculated results of this paper; points, experimental results of Ref. 31.

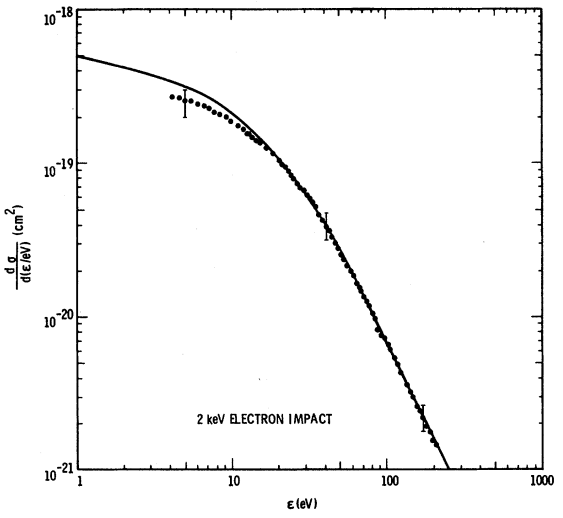

FIG. 5. Single differential cross section (SDCS) for electrons ejected from He by 2-keV electron impact as a function of ejected-electron energy ϵ. Solid curve, our calculated results; points, experimental results of Ref. 31.

sults on excitation using quantum-defect theory. They obtain a value of $d\sigma/d\epsilon|_{\epsilon=0} = 4.31\times10^{-19}$ cm^2 for 2-keV electron impact, compared with our results of 5.2×10^{-19} cm^2 and the (extrapolated) experimental result of 3.4×10^{-19} cm^2. Thus, it seems that the true value lies about halfway between the theoretical and experimental results given in Fig. 5.

From the above comparisons, we conclude that the Born approximation is excellent for 2-keV electron-impact ionization of He *provided decent wave functions are used for initial discrete and, especially, final continuum states,* except for ejected-electron energies below about 13 eV, where our SDCS result seems to be about 20% too large. Subject to these limitations, this type of calculation should be at least this good for electron-impact ionization at energies above 2 keV. Since the matrix elements $R^{\lambda}_{nl_0,\epsilon l}(K)$ have already been calculated and are stored, it is a simple matter to compute the DDCS and SDCS for electron impact at higher energies. The authors would be happy to provide such results to anyone interested.

For impact energies below 2 keV much experimental data on He has been reported.[28-35] The utility of the Born approximation in predicting the DDCS and SDCS for lower-energy electron impact has not yet been tested. Such calculations are in progress and a report on the details of how the Born approximation, even with reasonably good wave functions, breaks down will be presented in the future.

B. 100-keV proton impact

Experimental data on DDCS for 100-keV proton-impact ionization of He have been reported by Rudd and co-workers.[14,15] In Figs. 6A–6D a comparison between the calculated and experimental DDCS results are shown for ejected electrons of energies 13.6, 40.8, 81.6, and 163.2 eV. The results of this comparison are quite different from the electron-impact results. For $\epsilon = 13.6$ eV (Fig. 6A), the experimental result is a *factor* of 4 larger than the theoretical at 10°, the smallest angle measured. From 10° to 50° the theoretical curve is rather flat whereas the experimental result drops so sharply that both agree at $\theta \sim 50°$. Above 50° the experimental DDCS drops below the theoretical and remains there out to 160° (the largest angle measured). The shapes of the curves in the 50°–180° region are, however, exactly the same, including the slight rise of the cross section at backward angles. At ejected-electron energy $\epsilon = 40.8$ eV (Fig. 6B) the experimental result is a factor of 8 larger than the theoretical at 10° and, like the $\epsilon = 13.6$ eV comparison, the agreement is excellent by $\theta \sim 50°$. Again this occurs because the experimental result falls rapidly while the theoretical experiences only a slight increase in going from 10° to 50°. In the 50°–180° range, however, agreement remains excellent, unlike the 13.6-eV data. Going up in electron energy to $\epsilon = 81.6$ eV (Fig. 6C) the situation is substantially the same as at $\epsilon = 40.8$ eV except that now the experimental result is only a factor of 3 larger than the theoretical DDCS at 10° and the two results agree well from 40° on out. For $\epsilon = 163.2$ eV (Fig. 6D) very good agreement is obtained over the entire 0°–180° angular range.

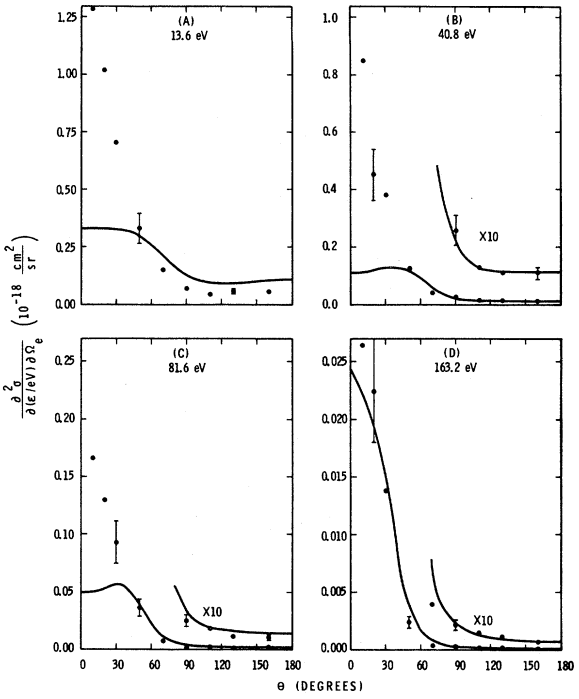

FIG. 6. Angular distribution (DDCS) for electrons ejected at 13.6, 40.8, 81.6, and 163.2 eV by 100-keV proton impact on He. Solid curves, calculated results of this paper; points, experimental results of Refs. 14 and 15.

The flattening or slight rise in both the theoretical and experimental DDCS for the backward angles is a consequence of the interference of continuum waves of different angular momenta and non-Coulomb phase shifts as discussed in connection with 2-keV electron impact in Sec. IV A. The agreement between theory and experiment is excellent at these angles, except for $\epsilon = 13.6$ eV, where the continuum wave functions employed in the calculation may be expected to be less accurate owing to the polarization of the ionic core by the slow outgoing electron, and experimental difficulties may also arise in detecting these slow electrons efficiently. We would, there-

fore, expect that at large angles an *exact* experiment and a Born theory with *exact* atomic wave functions (discrete *and* continuum) would show excellent agreement down to threshold, $\epsilon = 0$. At the backward angles BEA[39,54,55] and *hydrogenic* Born[36-38] DDCS are consistently too small by about an order of magnitude, for 100-keV proton impact. Thus, as expected from the electron-impact results in Sec. IV A, as well as from the work of Madison (Ref. 38), the use of a reasonable continuum wave function is crucial for the large-angle behavior of the DDCS.

At electron-ejection angles in the forward direction the agreement between theory and experiment is very poor for electron energies from 13.6 to 81.6 eV but fairly good for $\epsilon = 163.2$ eV. This is unlike the electron-impact results, where the agreement is uniformly good over the entire angular range. Qualitatively, the reason for this behavior has been explained in terms of a process of charge exchange from the target to the incident ion.[17,52,57,58] In the inelastic collision with the He atom the proton gives up only a very small fraction of its energy and thus the scattering angle is quite small, of the order of milliradians, and the protons go on basically undeflected. If a charge exchange process then occurs to a *continuum* state of hydrogen, these electrons would be detected primarily in the forward direction, the direction of motion of the proton. Further, the continuum electron resulting from the charge-exchange process will have the greatest probability of being produced at zero energy with respect to the proton. Thus, in the laboratory system, the greatest relative number of charge-exchange continuum electrons should be produced with a velocity equal to the proton velocity. For 100-keV protons, this corresponds to an electron energy $\epsilon \sim 54$ eV. This conforms with our results (Figs. 6A–6D) in which we see that at $\theta = 10°$, the experimental result is a factor of 8 times the theoretical at $\epsilon = 40.8$ eV, but only a factor of 4 at the lower energy of $\epsilon = 13.6$ eV and only a factor of 3 at the higher energy of $\epsilon = 81.6$ eV. In fact, for $\epsilon = 163.2$ eV the difference between theory and experiment is just about within experimental error although experiment may be as much as 30% above theory here. This process of continuum charge exchange shall be discussed and analyzed further in Sec. IV F.

The theoretical and experimental SDCS, or ejected-electron energy distribution, is shown in Fig. 7. Here it is seen that the agreement between theory and experiment is excellent above $\epsilon = 130$ eV but between $\epsilon = 10$ and 130 eV the theoretical result is significantly smaller than the experimental. The (percentage) difference is greatest

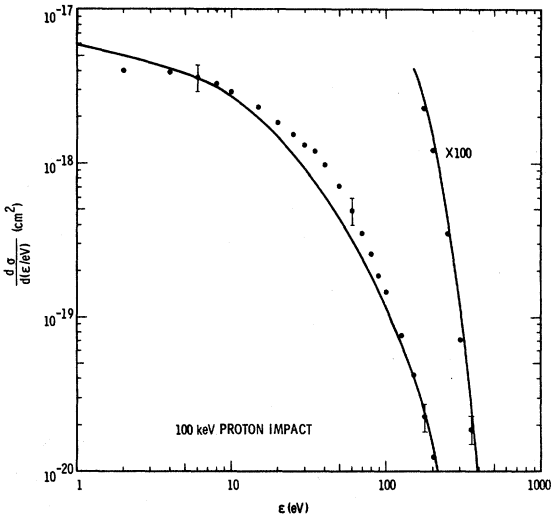

FIG. 7. Single differential cross section (SDCS) for electrons ejected from He by 100-keV proton impact as a function of ejected electron energy ϵ. Solid curve, our calculated results; points, experimental results of Refs. 14 and 15.

in the range $\epsilon = 30$–60 eV. This is entirely consistent with the above discussion, which suggested that the maximum discrepancy should occur when electron and proton velocities are equal or $\epsilon = 54.5$ eV. Note, however, that at worst the experimental SDCS is 70% above the theoretical while for the DDCS we found discrepancies as large as a factor of 8 at small angles. This is because the DDCS is the cross section per unit solid angle and the integration over solid angle to obtain the SDCS introduces a factor of $\sin\theta$ since $d\Omega = \sin\theta\, d\theta\, d\phi$. This factor reduces significantly the contribution to the SDCS of the angles 0°–30°, where the continuum charge-exchange effect is largest. Thus, the discrepancies between theory and experiment in the SDCS are much smaller than those in the DDCS.

For $\epsilon = 10$ eV the theoretical SDCS rises above the experimental. The charge-exchange mechanism should still be operative here and we can find no other physical effect which would make the results behave in this way. We thus conclude that the theoretical result is probably high (as it was in the electron-impact case) due to the polarization effects neglected in the calculation. It is also possible that the experimental result is somewhat low owing to difficulties in detecting low-energy electrons. The question is presently unresolved.

C. 300-keV proton impact

Experimental DDCS data for 300-keV proton-impact ionization of He have been reported by

Rudd *et al.*[15] In addition, 300-keV proton-impact data have been obtained at BNW and at HMI which were found to be in good agreement with each other and with the Rudd *et al.*[15] data for ejected-electron energies of 10 eV and above. This agreement is shown in Figs. 1 and 2 and discussed in Sec. III. In view of this, comparisons have been made between the theoretical DDCS and the experimental results of Rudd *et al.*[15] The resulting comparisons are given for $\epsilon = 13.6$, 40.8, 81.6, and 163.2 eV in Fig. 8A–8D and for $\epsilon = 326.4$ eV in Fig. 9. These show a similar situation to what we found for the 100-keV proton-impact results discussed in Sec. IVB: For the smaller angles, the theoretical results are substantially smaller in each case, while for large angles, agreement is quite good for all of the electron energies considered. For $\epsilon = 13.6$ eV (Fig. 8A) the experimental data are a factor of 3 larger than the theoretical DDCS at $\theta = 10°$. The experimental DDCS falls rapidly with increasing angle while the theoretical curve rises slightly so that they are within the experimental uncertainties by $\theta = 70°$. At the larger angles, experiment lies slightly below theory, but not nearly as much as in the 100-keV case. The rise of the DDCS for $\epsilon = 13.6$ eV at backward angles above 130° is seen both theoretically *and* experimentally, further confirming that the large-angle behavior of the DDCS is well

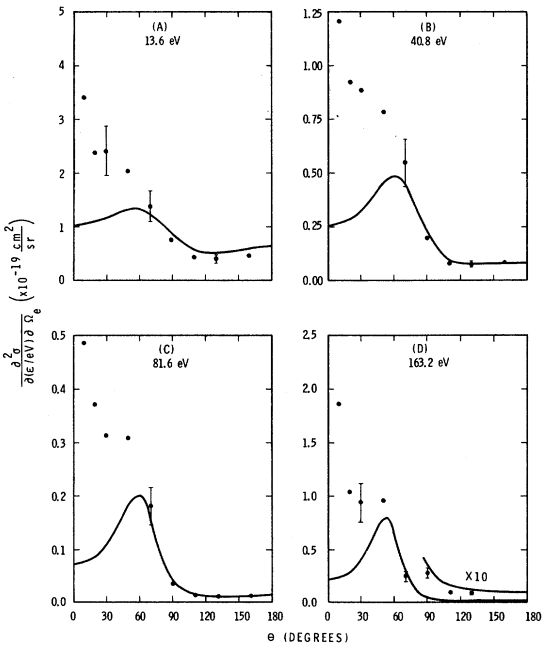

FIG. 8. Angular distribution (DDCS) for electrons ejected at 13.6, 40.8, 81.6, and 163.2 eV by 300-keV proton impact on He. Solid curves, calculated results of this paper; points, experimental results of Ref. 15.

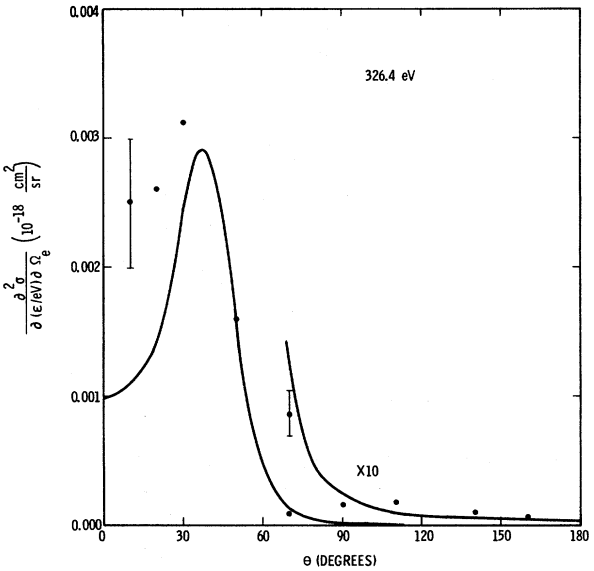

FIG. 9. Angular distribution (DDCS) for electrons ejected at 326.4 eV by 300-keV proton impact on He. Solid curve, calculated result of this paper; points, experimental results of Ref. 15.

represented by Born approximation. Note, however, that theory and experiment do not agree until $\theta = 70°$ as opposed to $\theta = 50°$ for the 100-keV results at the same electron energy. This implies that the continuum charge-exchange effect is greater at the larger angles for 300 keV than for 100 keV.

At $\epsilon = 40.8$ eV (Fig. 8B) the experimental DDCS is almost a factor of 5 greater than the theoretical at $\theta = 10°$. Again, they are equal, within experimental uncertainties, at $\theta = 70°$ (as opposed to 50° for 100-keV protons) and excellent agreement is seen in the region of the slightly increasing backward tail. The data for $\epsilon = 81.6$ eV (Fig. 8C) shows that experiment is more than 5 times larger than theory at $\theta = 10°$ but by $\theta = 70°$ ($\theta = 40°$ for 100 keV) they are equal and remain so for all larger angles. At $\epsilon = 163.2$ eV (Fig. 8D) the experimental DDCS is more than 9 times the theoretical at $\theta = 10°$ but they are in good agreement from $\theta = 50° - 180°$. Finally, for $\epsilon = 326.4$ eV (Fig. 9) experiment is only slightly more than a factor 2 larger at $\theta = 10°$ and good agreement between theory and experiment is found from $\theta = 40°$ on out.

In these results (Figs. 8 and 9) we see that experiment and theory agree well at large angles, further confirming the influence of the non-Coulomb phase shifts on the large-angle DDCS. At small angles the charge-exchange mechanism predominates and it is expected that this will be greatest when the ejected electron has the same

velocity as the proton, 163.4 eV in this case. This is indeed what we find in our results: the ratio of the experimental to the theoretical DDCS for electron energies of 81.6, 163.2, and 326.4 eV, respectively, are approximately 5, 9, and 2 at $\theta = 10°$.

The energy distribution of ejected electrons (SDCS) for 300-keV proton impact is given in Fig. 10. From $\epsilon = 350$ eV and above, the agreement between theory and experiment is excellent. For smaller electron energies, the effects of the continuum charge-exchange process are clearly seen with the experimental SDCS about 50–60% above the theoretical in the 50–200-eV region. Note that this contribution is somewhat less than the maximum 70% found for 100-keV proton impact. This implies that the cross section for the charge-exchange mechanism is falling off relative to the direct Coulomb ionization mechanism.

For very low electron energies, experiment again falls below theory (as it did for the 100-keV data) and we regard this as a failing in the calculation and/or the measurement but, at this point, we cannot say which.

D. 1-MeV proton impact

The DDCS for 1-MeV proton-impact ionization of He has been measured and calculated. The experimental results for ejection angles θ from 15° to 125° are shown in Fig. 11. We estimate the over-all accuracy of this data[18] to be ± 20%, although it is probably better around the peaks of the angular distribution and somewhat poorer on the wings at the larger angles, particularly at the higher electron energies where the DDCS drops more than two orders of magnitude from the maximum to the wings. The experimental data were smoothed where statistical scatter was significant.

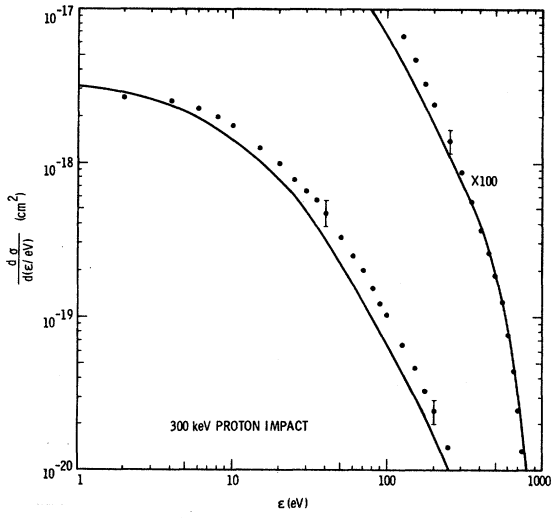

FIG. 10. Single differential cross section (SDCS) for electrons ejected from He by 300-keV proton impact as a function of ejected electron energy ϵ. Solid curve, our calculated results; points, experimental results of Ref. 15.

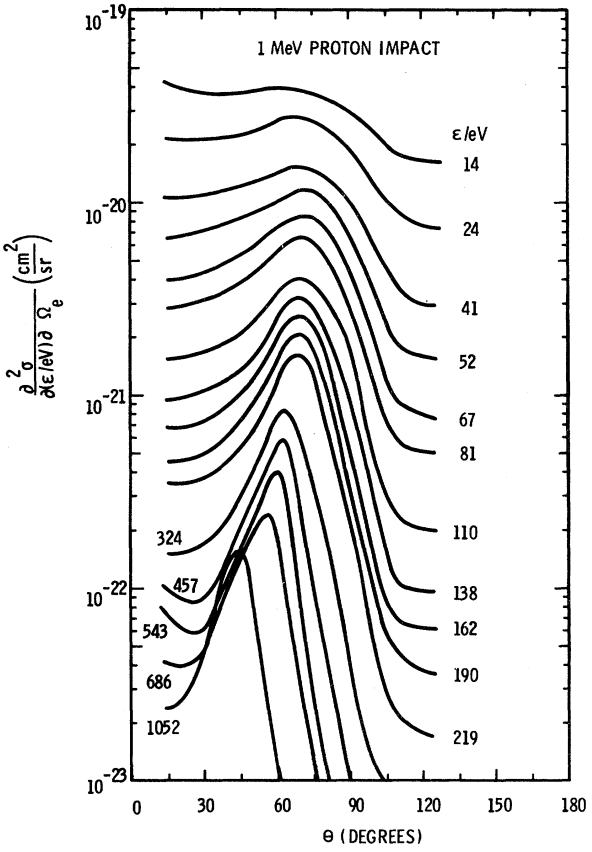

FIG. 11. Experimental angular distribution (DDCS) for electrons ejected at energies ϵ/eV from 14 to 1052 eV by 1-MeV proton-impact ionization of He performed at BNW.

The results from $\epsilon = 14$ eV to $\epsilon = 1052$ eV show the same sort of increased peaking, with increasing ϵ, as was shown by our electron-impact results (Sec. IV A). This was not seen very clearly for the 100- and 300-keV proton-impact ionization results owing to the huge effects of the continuum charge-transfer process at those energies. For 1-MeV protons, the effect is not nearly so dominant, compared to direct Coulomb ionization, although it is still in evidence. As discussed previously, the continuum charge-exchange mechanism should be at its maximum relative to direct Coulomb ionization when the electron and proton velocities are equal. For 1-MeV proton impact this occurs for ejected electrons of energy $\epsilon = 544$ eV. The results in Fig. 11 show the maxi-

mum relative increase in the forward direction (actually at $\theta = 15°$ since this is as close to the forward direction as the apparatus could measure) is at 543 eV, confirming this expectation.

We also note from Fig. 11 that the DDCS for a given angle is not monotonically decreasing as a function of ϵ for large ϵ; for example, at $\theta = 40°$, the DDCS is greater for $\epsilon = 1052$ eV than for $\epsilon = 686$ eV. This is a consequence of the binary-encounter peak moving to smaller θ as the ejected-electron energy increases. Thus, while the total probability for ejecting an electron with $\epsilon = 1052$ eV decreases relative to $\epsilon = 686$ eV, the ejection occurs primarily at a smaller angle leading to a rise in the DDCS at that angle. This phenomenon will continue to occur for still higher energies of ejection. Our 1-MeV proton-impact ionization measurements have been made for ϵ up to 2.5 keV. These higher-energy points were not included since they would clutter up the figure without adding further significance; nevertheless, the authors would be happy to make these results available to any interested readers. Note also, that data have been taken with a much finer energy mesh than is presented in Fig. 11. This, too, is available upon request.

The angular distributions of the DDCS results presented in Fig. 11 flatten out at the backward angles, similar to what was found both experimentally and theoretically for electron-impact and 100- and 300-keV proton-impact ionization. Owing to the limitations of the experimental apparatus, however, measurements could only be made out to $\theta = 125°$. We thus cannot infer from these results whether the DDCS merely becomes flat (as a function of θ) in the backward region, or if it rises again in going to $\theta = 180°$.

The experimental DDCS results are compared with our calculated values in Figs. 12 for $\epsilon = 13.6$, 40.8, 81.6, 163.2, 326.4, and 652.8 eV. The experimental points in Fig. 12A–12F represent the average of two separate measurements. For $\epsilon = 13.6$ eV (Fig. 12A) the experimental DDCS is a factor of only 1.5 times the theoretical at 15°, a much lower fraction than for 300-keV protons. Above about 30°, however, agreement is fairly good. The discrepancies at the larger angles are slightly larger than the experimental uncertainties but this is not surprising at such a low electron energy. As discussed previously, the shapes of both theoretical and experimental curves at large angles are similar and theory predicts a subsequent rise in the DDCS at $\theta = 180°$. The experimental DDCS was not measured at large enough angles to confirm or deny this prediction. In any case, the comparison for small angles shows that the charge-exchange mechanism has decreased markedly in importance, relative to direct Coulomb ionization, compared to 300-keV proton impact.

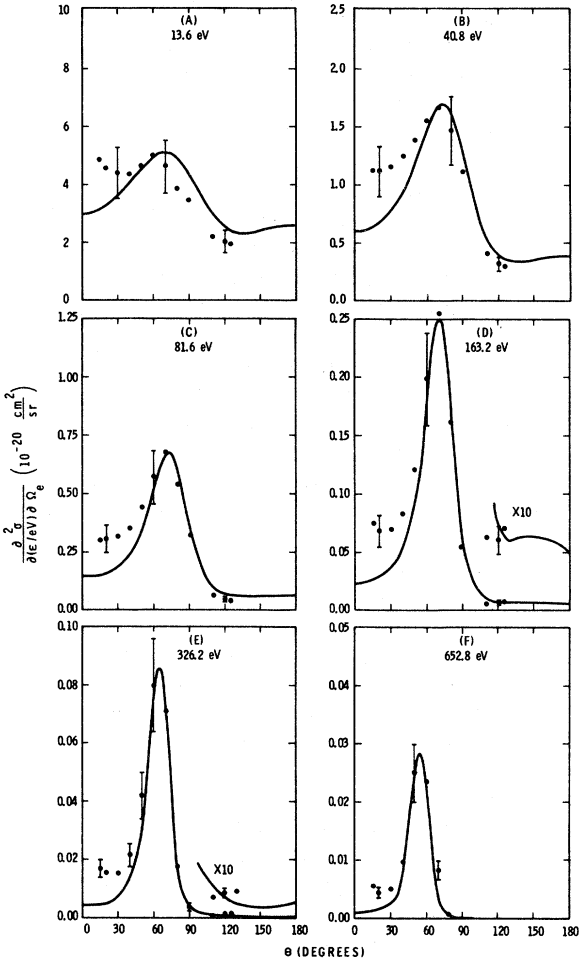

FIG. 12. Angular distribution (DDCS) for electrons ejected at 13.6, 40.8, 81.6, 163.2, 326.4, and 652.8 eV by 1-MeV proton impact on He. The solid curves are our calculated results and the points are our experimental results measured at BNW.

At $\epsilon = 40.8$ eV (Fig. 12B) the ratio of experiment to theory is 1.8 at 15°. The two results come together at $\theta \sim 50°$ and agreement is quite good from there on out in angle. Again, the theory predicts an upward tailing of the DDCS at the backward angles, but the experiment does not go out that far in angle.

The $\epsilon = 81.6$ eV results (Fig. 12C) show a ratio of experiment to theory of 2 at $\theta = 15°$. The curves come together at 60° and agreement is good for $\theta > 60°$. For $\epsilon = 163.2$ eV (Fig. 12D) the ratio is 3 at $\theta = 15°$, and agreement is excellent for all $\theta > 60°$. At $\epsilon = 326.4$ eV (Fig. 12E) the $\epsilon = 15°$ ratio is 4 and excellent agreement occurs for $\theta > 50°$. Finally, the $\epsilon = 652.8$-eV results (Fig. 12F) also

have a 15° ratio of 4 and agreement is excellent at and above $\theta = 40°$. Data are not shown above $\theta = 90°$ because the cross section becomes so small; both the experiment and the calculation become unreliable.

The results in Fig. 12A–12F show that the relative importance of the continuum charge-exchange mechanism maximizes between $\epsilon = 326.4$ and 652.8 eV. This is consistent with our expectations and the results shown in Fig. 11, both of which pointed to the relative maximum being at about $\epsilon = 544$ eV. The over-all relative strength of the continuum charge-exchange effect is seen to be much less than for the lower-energy protons discussed in Secs. IV B and IV C. This implies that at high enough proton energy, the only significant production of continuum electrons will be the direct Coulomb ionization mechanism and the Born approximation (with reasonable wave functions) will predict the DDCS quite well. This point shall be discussed in greater detail in Sec. IV F.

Experimental and theoretical results for the SDCS are given in Fig. 13. The experimental results lie somewhat below the theoretical for electron energies below about 30 eV. For $\epsilon > 30$ eV, however, the theoretical results are slightly higher (5–10%) but the agreement over the entire range is well within the ±20% estimated experimental uncertainty. Thus, to within experimental uncertainty, we see no effects of the continuum charge-exchange mechanism in the SDCS; at the point where it would be expected to maximize, $\epsilon = 544$ eV, the experimental SDCS is only about 5% greater than theory, which is much smaller than the ±20% experimental uncertainty. We conclude then, that for 1-MeV proton impact our calculation of the SDCS is good and the continuum charge-exchange mechanism is small enough to be neglected. This, however, is not the case for the DDCS, as we have shown in Fig. 12. The lessening in relative importance of the continuum charge-exchange process in going from the DDCS to the SDCS is a consequence of (i) the fact that the peak of the experimental DDCS for 1-MeV proton impact is now at the binary-encounter peak, rather than at $\theta = 0°$ as was found for 100- and 300-keV proton impact, and (ii) the $\sin\theta$ factor in the $d\Omega$ integration diminishes the importance of anything at small angles.

E. 5-MeV proton impact

Theoretical and experimental results have been obtained for the DDCS from 5-MeV proton-impact ionization of He. The ejection angles measured were from $\theta = 25°–150°$ and the experimental DDCS

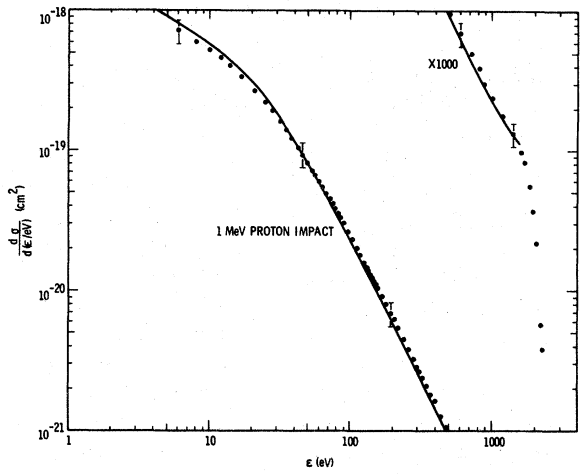

FIG. 13. Single differential cross section (SDCS) for electrons ejected from He by 1-MeV protons as a function of electron energy ϵ. The solid curve is our calculated results and the points are the results of our experiments performed at BNW.

results are presented in Fig. 14. As in the case of 1-MeV proton impact, we estimate experimental uncertainties to be ±20% with better accuracy at the peaks of the angular distributions than on the wings. The curves drawn represent smoothed results where statistics were poor and scatter was significant.

The 5-MeV proton-impact ionization DDCS for ejected electrons with $\epsilon = 6.8$ eV to $\epsilon = 1166$ eV present an over-all picture similar to the 1-MeV results. The angular distributions become more and more peaked about the binary-encounter peak with increasing ϵ and this feature dominates the DDCS. A major difference between these results and those for lower proton energies is the absence of even a hint of peaking at the forward angles, i.e., we find no evidence for any sizable effects from the continuum charge-exchange process. We would expect this process to maximize relative to the direct ionization process for $\epsilon = 2720$ eV (not shown in Fig. 14), where the ejected electron and the 5-MeV proton have the same velocity. However at such a large electron energy, the DDCS is too small at the forward angles to be separated from the background. We note parenthetically that measurements have been made for ϵ up to 7.5 keV and for a much finer ϵ mesh than is shown in Fig. 14. These data are available from the authors to anyone interested.

As in the case of the 1-MeV proton-impact data, it is seen from Fig. 14 that the DDCS is not monotonically decreasing as a function of ϵ for a given θ. For the largest ϵ shown, e.g., at $\theta = 60°$, the DDCS is greater for $\epsilon = 1166$ eV than for $\epsilon = 858$

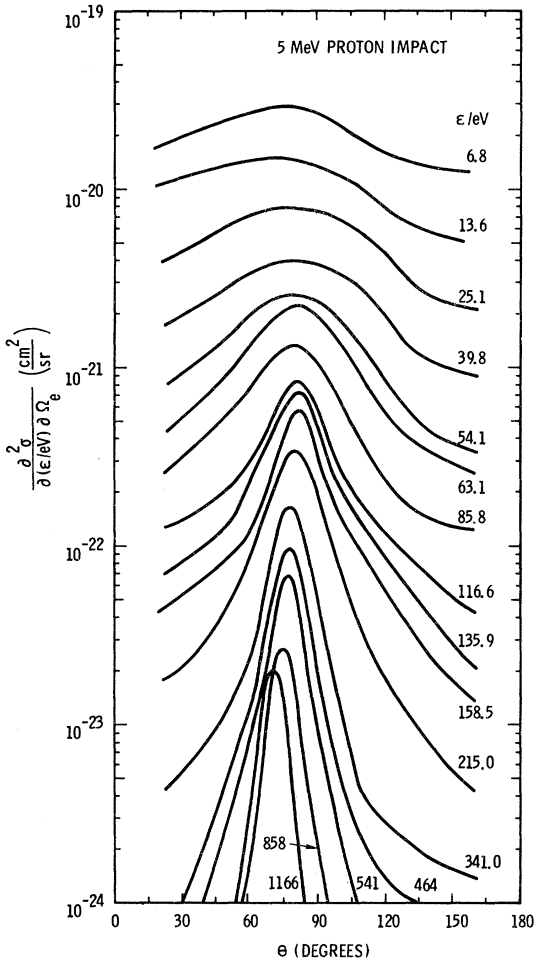

FIG. 14. Experimental angular distribution (DDCS) for electrons ejected at energies ϵ/eV from 6.8 to 1166 eV by 5-MeV proton-impact ionization of He performed at HMI.

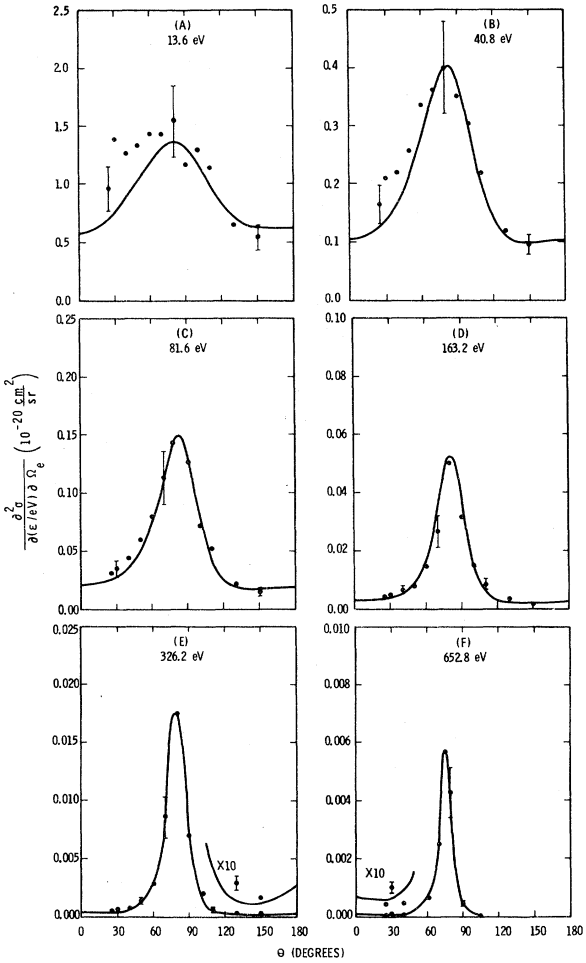

FIG. 15. Angular distribution (DDCS) for electrons ejected at 13.6, 40.8, 81.6, 163.2, 326.4, and 652.8 eV by 5-MeV proton impact on He. The solid curves are our calculated results and the points are our experimental results measured at HMI.

eV. The explanation for this, in terms of the kinematics of the collision causing the binary-encounter peak to move to smaller angles, as ϵ increases is exactly the same as in the 1-MeV case which is discussed in Sec. IV D.

We compare the above experimental results with our calculated DDCS data in Fig. 15 A–15 F for $\epsilon = 13.6$, 40.8, 81.6, 163.2, 326.4, and 652.8 eV. Here the experimental points are the actual measured values with no smoothing. For $\epsilon = 13.6$ eV (Fig. 15A) the experimental data show significant scatter. This has been found to be generally true for ejection of 13.6-eV electrons, as was observed in the preceding sections for the lower proton energies and for electron impact. Agreement between the experimental and theoretical DDCS results is fairly good despite this. At the smaller angles, the experimental DDCS lies above the theoretical but not in such a way as to indicate the effects of the continuum charge-exchange mechanism; i.e., the experimental data do not diverge from the theoretical with decreasing θ but remain systematically above. Thus, we conclude that either the experimental DDCS is too large at $\epsilon = 13.6$ eV or the theoretical is too small, but in neither case can the difference be attributed to the effects of continuum charge transfer.

At $\epsilon = 40.8$ eV (Fig. 15 B) the agreement is quite good between calculated and measured cross sections at all angles, differences being essentially within experimental uncertainty except for the points at $\theta = 25°$ and 30°. If these differences were, in fact, a manifestation of the charge-exchange process, it should be more significant as ϵ increases. We see, however, just the opposite ef-

fect. For $\epsilon = 81.6$ eV (Fig. 15C) agreement is excellent over the entire angular range measured. This reinforces our argument that discrepancies at the lower energies do not result from continuum charge exchange. We also see quantitative confirmation of the theoretical prediction of a flattening of the angular distribution at the backward angles. Unfortunately the measurements have not been made at large enough angles to see the backward rise predicted by theory.

At $\epsilon = 163.2$ eV (Fig. 15D) agreement again is excellent over the entire angular range and this is also the case for $\epsilon = 326.4$ eV (Fig. 15E). The $\epsilon = 652.8$-eV comparison (Fig. 15F) shows serious experimental scatter on the small-angle side of the peak, and on the high-angle side, the DDCS becomes so small that both the calculation and the measurement become extremely unreliable. However, the agreement in the vicinity of the binary-encounter peak is excellent.

From the comparisons in Fig. 15A–15F, it is seen that, for 5-MeV proton-impact ionization of He, no evidence for the occurrence of a continuum charge-exchange process exists, to within experimental error. It is, of course, possible that it is only operative at electron ejection angles smaller than $\theta = 25°$, but based on our results for 100-keV, 300-keV, and 1-MeV proton impact, it seems likely that if the charge-exchange mechanism were important at $\theta = 0°$, its effects would be apparent in the $\theta = 25° - 50°$ range as well. Therefore, we conclude that the direct Coulomb ionization process is the only mechanism of significance in producing continuum electrons for 5-MeV protons on He.

Integrating the DDCS over ejected-electron angles, we obtain the SDCS or ejected-electron energy distribution. Theoretical and experimental results are shown in Fig. 16, where we see excellent agreement for electron energies of 15 to about 500 eV. This is a further confirmation of the nonimportance of the charge-exchange effect for 5-MeV proton-impact ionization. Above 500 eV, the experimental SDCS falls below the theoretical curve despite the fact that we found excellent agreement in the DDS at $\epsilon = 652.8$ (Fig. 15F). The difficulty here lies in the integration of the experimental DDCS over angle. The data were taken in 10° steps and, as seen from Fig. 15F, no experimental point was taken at the top of the narrow binary-encounter peak. Thus, it is clear that the numerical integration of the experimental DDCS will be too small. To get around this difficulty, it is necessary to take data at very closely spaced angular intervals around the binary peak so that the integral can be performed accurately.

At the low energies, it is seen from Fig. 16 that the experimental points lie below the calculated

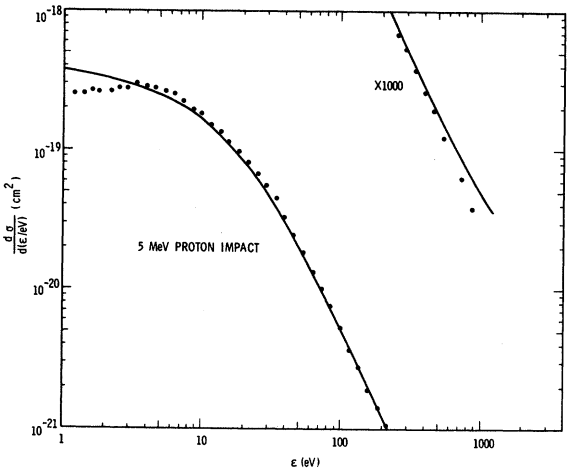

FIG. 16. Single differential cross section (SDCS) for electrons ejected from He by 5-MeV protons as a function of electron energy ϵ. The solid curve is our calculated results and the points are the results of our experiments at HMI.

values. This is similar to what has occurred for 2-keV electron impact and the lower-energy proton impact. For reasons discussed previously, it is expected that the theoretical SDCS is somewhat high for small ϵ and it is experimentally difficult to obtain accurate cross sections for $\epsilon \leq 10$ eV.

F. Continuum charge-exchange process

From the presentations in Secs. IV A–IV E, it is clear that an important contribution to the ejected-electron spectrum resulting from 100- and 300-keV proton-impact ionization of He arises from the continuum charge-exchange process. The relative importance of this effect was seen to be much smaller for 1-MeV proton impact and had essentially disappeared for 5-MeV proton impact. Further, from the qualitative explanation of this effect (Sec. IV B) it was clear that the electrons ejected by the charge-exchange process would exit primarily in the same direction as the incident proton beam, i.e., small angles in the laboratory. The experimental results indicated that this, indeed, was the case. Even for proton-impact energies of 100 and 300 keV, the agreement between the experimental and theoretical DDCS was excellent at large angles (in the laboratory), where the charge-exchange mechanism was unlikely to produce many electrons. Thus, the Born approximation, with reasonable wave functions, predicts the large-angle behavior of the DDCS down to proton-impact energies at least as low as 100 KeV. As far as the Born approximation treatment of the direct Coulomb ionization mechanism is concerned, there should be no systematic angular dependence

of the accuracy. Thus we conclude, and the rest of the analysis of this section is predicated upon this conclusion, that the predictions of the Born approximation are an accurate representation of the direct Coulomb ionization mechanism at all angles. Within this assumption deviations between theory and experiment at small angles are the result of another process, the continuum charge-exchange mechanism, and are *not* symptomatic of the breakdown of the Born-approximation treatment of direct Coulomb ionization. Keeping this conclusion in mind, then, we proceed to a quantitative analysis of the dependence of the continuum charge-exchange process on the incident-proton energy.

From the discussion of the continuum charge-exchange mechanism in Sec. IV B, as well as from succeeding comparisons between experimental and theoretical DDCS results, we have seen that the relative importance of this effect is greatest at forward angles and for ejected-electron energies such that the electron velocity (V_e) and proton velocity (V_p) were equal. To obtain quantitative information on how the relative magnitude of the continuum charge-exchange process decreases with increasing proton energy, we have calculated the ratio of the experimental to theoretical DDCS at a number of the forward angles for $V_e = V_p$. Since the experiment measures the sum of the electrons ejected by direct Coulomb ionization *and* by continuum charge exchange, while the theoretical prediction is a fairly accurate determination of the DDCS for direct ionization alone, this ratio gives a reasonable estimate of the relative magnitude of continuum charge-exchange contribution. The results are shown in Fig. 17 with the ratio plotted versus proton energy for $V_e/V_p = 1$. From this figure, it is seen that the ratio approaches unity at higher proton energies for all of the angles considered. Further, the maximum in the ratio lies between 300 and 500 keV and moves to higher proton energy with decreasing angle. In addition, the magnitude of the maximum in the ratio increases markedly with decreasing angle. It is noteworthy that at the lower proton energies, Fig. 17 shows that even at $\theta = 50°$, the charge-exchange contribution to the DDCS can be as much as 30% of the direct ionization, i.e., a ratio of as large as 1.3.

The fact that the ratio approaches unity for all angles shown with increasing proton energy further substantiates our assertion that the Born approximation, with Hartree-Slater wave functions, does indeed predict reasonably accurate results for the direct Coulomb ionization process. Unfortunately, we could not investigate the ratio for $\theta = 0°$ owing to experimental limitations cited earlier. A limited

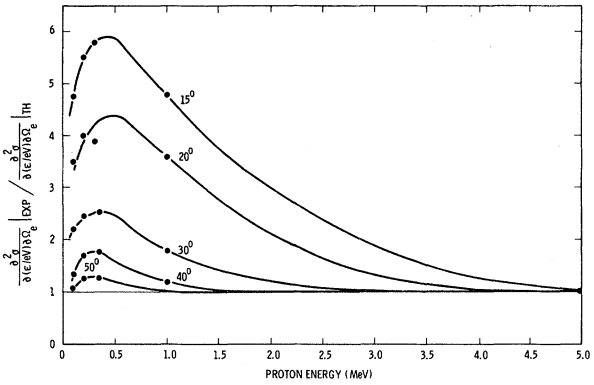

FIG. 17. Ratio of experimental to theoretical double differential cross section (DDCS) for protons on He for equal velocity incident protons and ejected electrons, shown vs proton energy for various ejection angles.

amount of data at $\theta = 0°$ has been obtained, but only for proton energies in the range 100–300 keV.[17] However, a more extensive investigation of the small-angle region is presently in progress.[59]

We can also obtain information on the actual cross sections for the continuum charge-exchange process by taking differences, rather than ratios, between the experimental and theoretical DDCS. These differences are shown for $V_e/V_p = 1$ in Fig. 18, where the results are given for proton energies of up to 1 MeV; at 5 MeV the differences are too small to be meaningful. The curves shown in Fig. 18 all approach the same slope of about -5 at the higher proton energies, which means that the double differential continuum charge-exchange cross sections go roughly as T^{-5} (T is the proton energy). This observation is entirely consistent with the measured asymptotic dependence of the cross section for charge exchange to the ground state of the proton-electron system (hydrogen atom).[60] Thus we find that the assumption of the continuum charge-exchange mechanism is entirely consistent with previous charge-exchange work.

In closing this section, we note that two different theoretical treatments have been reported which treat the proton-impact ionization of He including the continuum charge-exchange process[57,58] and that both agree *qualitatively* with experimental results. To get good quantitative agreement, one would probably have to include the "quasimolecular" nature of the system when the colliding particles are close in addition to having a reasonably correct asymptotic form for the wave function. A recent, fairly successful, attempt in this direction has been made by Band.[61] Since the quasimolecular aspects of a collision are very dependent upon the charge of the incident particle,[62]

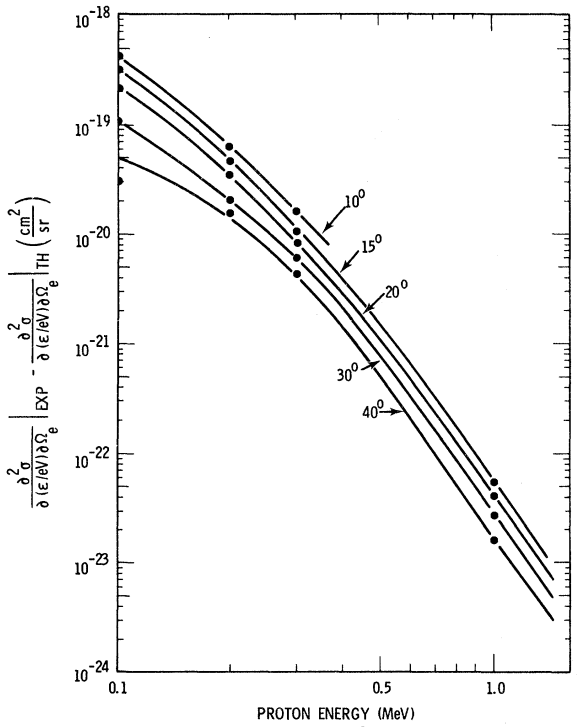

FIG. 18. Difference between experimental and theoretical double differential cross section (DDCS) for protons on He for equal velocity incident protons and ejected electrons, shown vs proton energy for various ejection angles.

a measurement of the DDCS for α-particle impact ionization of He would be useful.

V. CONCLUDING REMARKS

This paper has presented a comprehensive study of the ejection of electrons in collisions of fast electrons and protons with He. New experimental results for 300-keV, 1-MeV, and 5-MeV proton impact have been reported along with theoretical results for 2-keV electron impact and proton-impact energies of 100 keV, 300 keV, 1 MeV, and 5 MeV. From these results we have found that the results of the Born approximation using realistic wave functions were excellent for the 2-keV electron-impact DDCS and SDCS, except perhaps for very-low-energy ejected electrons ($\epsilon \leq$ eV). For proton impact, we found, as was found previously,[38] that for 100- and 300-keV incident energies serious discrepancies between theory and experiment exist in the DDCS for small (forward) angles of ejection. This discrepancy was found to be much smaller for 1-MeV proton impact and was absent from the 5-MeV proton impact results. On the other hand, for the large (backward) electron-ejection angles, agreement between theoretical and experimental DDCS was uniformly good as was also found in Ref. 38. This indicated that the large-angle discrepancies found in earlier Born-approximation calculations[36] were *not* due to inadequacies in the Born approximation but rather to the inaccurate continuum wave functions employed.

The explanation for the small-angle discrepancy in the DDCS for proton impact was ascribed to a shortcoming in the theoretical description of the process; the theory did not include the channel for charge exchange to the continuum which has been discussed by a number of workers.[52] We believe, for a number of reasons, that the Born approximation does, however, provide an adequate description of the direct ionization process. Thus, the difference between the experimental and theoretical DDCS was studied and it was found to have a proton-impact-energy dependence very similar to that of ordinary discrete charge-exchange cross sections. This further reinforces the assignment of the small-angle discrepancies to the continuum charge-exchange process.

It has been found previously,[38] and is further confirmed by the results of this paper, that the continuum charge-exchange effect becomes negligible when the *relative* electron-proton velocity is greater than 0.8–0.9 of the proton velocity. In this paper we have further found that the charge-exchange effect is negligible (compared to direct ionization) for proton energies of 5 MeV. Thus, while the above gives quantitative limits on the contribution of continuum charge exchange to the proton-impact ionization process, it is clear that further experimental and theoretical work is needed to fully clarify the situation.

In view of the results of this paper, the theoretical formulation used is probably quite adequate for the DDCS and SCDS for higher-energy (> 2 keV) electron-impact ionization and higher-energy (> 5 MeV) proton-impact ionization of He. Such calculations are in progress and will be reported shortly. In addition, experimental DDCS data for lower energy electron impact ionization of He are available[28-35] and calculations are underway to investigate the validity of the Born approximation in this region; recent experimental DDCS data for lower energy proton impact are available[63] and calculations have been performed to check the situation. These will be reported shortly.

Finally, we are in the process of extending this work to the rest of the noble gases, Ne, Ar, Kr, and Xe, and this, too, will be reported shortly.

ACKNOWLEDGMENTS

The authors would like to thank Dr. M. E. Rudd of the University of Nebraska for providing us with

the details of his data, and Dr. Y.-K. Kim of Argonne National Laboratory for accurately determining the SDCS from the DDCS for the experimental 5-MeV proton-impact data. In addition, one of us (S.T.M.) would like to acknowledge the hospitality of the Battelle Pacific Northwest Laboratory, where a major portion of this paper was written under a NORCUS Faculty Research Appointment. We are indebted to U. Leithaüser and H. Gabler for their assistance in the experiments carried out at HMI.

---

*Supported in part by National Science Foundation Grant GP-38905, U. S. Army Research Office–Durham Grant DAHCO 4-74-G-0217, and U. S. Atomic Energy Commission Contract AT (45-1)-1830.

[1]H. A. Bethe, Ann. Phys. (Leipz.) 5, 325 (1930).
[2]H. A. Bethe, in *Handbuch der Physik*, edited by H. Geiger and K. Sheel (Springer, Berlin, 1933), Vol. 24/1, p. 273.
[3]U. Fano, Ann. Rev. Nucl. Sci. 13, 1 (1963).
[4]M. Inokuti, Rev. Mod. Phys. 43, 297 (1971).
[5]U. Amaldi, A. Egidi, R. Maroneri, and G. Pizella, Rev. Sci. Instrum. 40, 1001 (1969).
[6]H. Ehrhardt, M. Schulz, T. Tekaat, and K. Willmann, Phys. Rev. Lett. 22, 89 (1969).
[7]H. Ehrhardt, K. H. Hesselbacher, K. Jung, and K. Willmann, Case Studies At. Collision Phys. 2, 159 (1972).
[8]H. Ehrhardt, K. H. Hesselbacher, K. Jung, and K. Willmann, J. Phys. B 5, 1559 (1972).
[9]H. Ehrhardt, K. H. Hesselbacher, K. Jung, M. Schulz, and K. Willmann, J. Phys. B 5, 2107 (1972).
[10]H. Ehrhardt, K. H. Hesselbacher, K. Jung, E. Schubert, and K. Willmann, J. Phys. B 7, 69 (1974).
[11]R. Camilloni, A. Giardini, R. Tiribelli, and G. Stefani, Phys. Rev. Lett. 29, 618 (1972).
[12]E. Weigold, S. T. Hood, and P. J. O. Teubner, Phys. Rev. Lett. 30, 475 (1973).
[13]C. E. Kuyatt and T. Jorgensen, Phys. Rev. 130, 1444 (1963).
[14]M. E. Rudd and T. Jorgensen, Phys. Rev. 131, 666 (1963).
[15]M. E. Rudd, C. A. Sautter, and C. L. Bailey, Phys. Rev. 151, 20 (1966).
[16]J. B. Crooks and M. E. Rudd, Phys. Rev. A 3, 1628 (1971).
[17]G. B. Crooks and M. E. Rudd, Phys. Rev. Lett. 25, 1599 (1970).
[18]L. H. Toburen, Phys. Rev. A 3, 216 (1971).
[19]L. H. Toburen and W. E. Wilson, Phys. Rev. A 5, 247 (1972).
[20]L. H. Toburen and W. A. Glass, Radiat. Res. 50, 6 (1972).
[21]L. H. Toburen, *VIIth International Conference on the Physics of Electronic and Atomic Collisions, Abstracts of Papers* (North-Holland, Amsterdam, 1971), p. 1120.
[22]L. H. Toburen, Phys. Rev. A 9, 2505 (1974).
[23]S. T. Manson and L. H. Toburen, *VIIIth International Conference on the Physics of Electronic and Atomic Collisions, Abstracts of Papers* (Institute of Physics, Belgrade, 1973), p. 695.
[24]N. Stolterfoht, Z. Phys. 248, 81 (1971).
[25]N. Stolterfoht, Z. Phys. 248, 92 (1971).
[26]H. Ehrhardt and F. Linder, Z. Naturforsch. A 22, 444 (1967).
[27]H. Ehrhardt, K. H. Hesselbacher, K. Jung, M. Schulz, T. Tekaat, and K. Willmann, Z. Phys. 244, 254 (1971).
[28]W. K. Peterson, C. B. Opal, and E. C. Beaty, J. Phys. B 4, 1020 (1971).
[29]C. B. Opal, W. K. Peterson, and E. C. Beaty, J. Chem. Phys. 55, 4100 (1971).
[30]W. K. Peterson, E. C. Beaty, and C. B. Opal, Phys. Rev. A 5, 712 (1972).
[31]C. B. Opal, E. C. Beaty, and W. K. Peterson, At. Data 4, 209 (1972).
[32]D. A. Vroom and A. R. Comeaux, *VIIth International Conference on the Physics of Electronic and Atomic Collisions, Abstracts of Papers* (North-Holland, Amsterdam, 1971), p. 878.
[33]N. Oda, F. Nishimura, and S. Tahira, J. Phys. Soc. Jpn. 33, 462 (1972).
[34]S. Tahira and N. Oda, *VIIIth International Conference on the Physics of Electronic and Atomic Collisions, Abstracts of Papers* (Institute of Physics, Belgrade, 1973), p. 411.
[35]G. B. Crooks, Ph.D. dissertation (University of Nebraska, 1972) (unpublished).
[36]W. J. B. Oldham, Phys. Rev. 140, A1477 (1965).
[37]W. J. B. Oldham, Phys. Rev. 161, 1 (1967).
[38]D. H. Madison, Phys. Rev. A 8, 2449 (1973).
[39]T. F. M. Bonsen and L. Vriens, Physica 47, 307 (1970).
[40]M. E. Rudd, D. Gregoire, and J. B. Crooks, Phys. Rev. A 3, 1635 (1971).
[41]H. S. W. Massey and C. B. O. Mohr, Proc. R. Soc. A 140, 613 (1933).
[42]N. F. Mott and H. S. W. Massey, *The Theory of Atomic Collisions*, 3rd ed. (Oxford U. P., London, 1965), p. 489.
[43]S. Geltman, *Topics in Atomic Collision Theory* (Academic, New York, 1969), p. 36.
[44]A. Messiah, *Quantum Mechanics* (North-Holland, Amsterdam, 1966), Vol. II, p. 1054.
[45]Reference 44, p. 1061.
[46]W. Miller and R. Platzman, Proc. Phys. Soc. Lond. A 70, 299 (1957).
[47]S. T. Manson, Phys. Rev. A 6, 1013 (1972).
[48]F. Herman and S. Skillman, *Atomic Structure Calculations* (Prentice-Hall, Englewood Cliffs, N.J., 1963).
[49]S. T. Manson, Phys. Rev. 182, 97 (1969).
[50]S. T. Manson and J. W. Cooper, Phys. Rev. 165, 126 (1968).
[51]S. T. Manson, Phys. Rev. A 5, 668 (1972).
[52]M. E. Rudd and J. Macek, Case Studies At. Collision Phys. 3, 47 (1972).
[53]N. Stolterfoht, D. Schneider, and P. Ziem, Phys. Rev. A 10, 81 (1974).
[54]L. Vriens and T. F. M. Bonsen, J. Phys. B 1, 1123 (1968).
[55]D. Banks, L. Vriens, and T. F. M. Bonsen, J. Phys. B 2, 976 (1969).

[56]Y. K. Kim and M. Inokuti, Phys. Rev. A 7, 1257 (1973).
[57]A. Salin, J. Phys B 2, 631 (1969).
[58]J. Macek, Phys. Rev. A 1, 235 (1970).
[59]J. W. McGowan (private communication).
[60]L. H. Toburen, M. Y. Nakai, and R. A. Langley, Phys. Rev. 171, 114 (1968).
[61]Y. B. Band, J. Phys. B 7, 2557 (1974).
[62]F. T. Smith, D. G. Lorents, and R. E. Olson, in *Proceedings of the International Conference on Inner Shell Ionization Phenomena and Future Applications*, Atlanta, Georgia, 1972, edited by R. W. Fink, S. T. Manson, J. M. Palms, and P. V. Rao, CONF-720 404 (U. S. Atomic Energy Commission, Oak Ridge, Tenn., 1973), p. 1175.
[63]M. E. Rudd, C. A. Blocker, and G. L. Webster, Bull. Am. Phys. Soc. 19, 1183 (1974), and private communication.